A Study on the Reaction Kinetics of Dendrimerization by FT-IR Spectroscopy: Propagation of PAMAM Dendrimer on Silica Gel

Ruijiang Li and Jie Bu[†]

Institute of Chemical and Engineering Science,
Ayer Rajah Crescent Block 28 Unit 02-08, Singapore 139959, Republic of Singapore

Abstract−Solid-phase PAMAM dendrimer was synthesized by the repetitive addition of a branching unit to silica gel. All synthesis steps were monitored by infrared spectroscopy to investigate the reaction rate. Based on the measurements of infrared spectra, which showed the ester group varied as a function of reaction time, a reaction kinetics model was proposed and simulated. FT-IR and TGA measurements suggested that a 'cross-linking' reaction occurred in amidation process and generated structural defects, which decreased the grafted amount of dendrimer on silica gel. In addition, the analysis of reaction rate constants indicated that due to the formation of an intermediate, Michael addition of methyl acrylate to diamine was probably hindered by steric crowding.

Key words: PAMAM Dendrimer, Silica Gel, Grafting, Solid Phase, FT-IR, Reaction Kinetics, Structure Defect

INTRODUCTION

Dendrimers are cascade-branched, highly defined macromolecules, characterized by a combination of high end group functionality and compact molecular structures. Since the seminal works in this field, a large number of dendrimer structures have been developed and it has become a subject of intense interdisciplinary research efforts, bringing together scientists from entirely different areas [Vogtle et al., 2000; Hecht and Frechet, 2001; Oosterom et al., 2001; Choi et al., 2002; Stiriba et al., 2002; van Heerbeek et al., 2002; Zimmerman et al., 2002; Bertorelle et al., 2003; Jang et al., 2003].

Polyamidoamine dendrimers (PAMAM) represent an exciting new class of macromolecular architecture called "dense star" polymers which have a high degree of molecular uniformity, narrow molecular weight distribution, specific size and shape characteristics, and a highly-functionalized terminal amino groups. The structural precision of PAMAM dendrimers has motivated numerous studies aimed at biomedical applications, for example, drug carriers [Beezer et al., 2003] and DNA delivery [Luo et al., 2002]. But since the synthesis of dendrimer is a series of repetitive steps starting with a central initiator core, the synthetic construction of dendrimers is tedious and time-consuming work. In addition, excess reagents are needed to drive reactions to completion which may render purification difficult. As a consequence, solid-phase synthesis has became a powerful tool in making PAMAM dendrimers, as excess reagents can be used to ensure complete reaction on solid surface and can be removed easily by simple washing.

Swali [Swali et al., 1997] described the synthesis of PAMAM dendrimers on the solid phase starting from a resin bead. An acid-labile linker attached to a polyamine scaffold was used to allow cleavage of the dendrimer from the resin in order to monitor the synthe-sis [Marsh et al., 1996]. On the other hand, grafting of PAMAM dendrimer on silica gel was reported [Tsubokawa et al., 1998]. Subsequently, silica supported PAMAM dendrimers have been widely investigated to explore its applications in catalysts [Bourque et al., 1999; Bu et al., 2003; Chung and Rhee, 2003] and chiral separation [Driffield et al., 2002]. However, incomplete reactions and structural defects were observed, especially in higher generations during synthesis of PAMAM dendrimer on solid phase [Tsubokawa et al., 1998; Bourque et al., 2000; Chung and Rhee, 2002]. So far there are not many investigations reported on monitoring the reactions, studying reaction kinetics, and controlling the level of structural defects for synthesis of PAMAM dendrimer. The purpose of this study is to monitor all synthesis steps by infrared spectroscopy to investigate the completion of reactions. Based on the experimental data, we intend to propose a reaction kinetics model. The structural defects will also be discussed.

EXPERIMENTAL

1. Materials and Reagents

To synthesize solid-phase PAMAM dendrimer, 3-Amino-functionalized silica gel (1.0 mmol NH₂/g, 30-80 μm) was used as starting material (G0) obtained from Sigma-Aldrich. It was dried in a tube oven at 110 °C before use. Methyl acrylate (MA) (Aldrich) was dried over sodium sulfate and distilled before use. Ethylendiamine (EDA) (J. T. Baker) was refluxed over sodium and distilled before use.
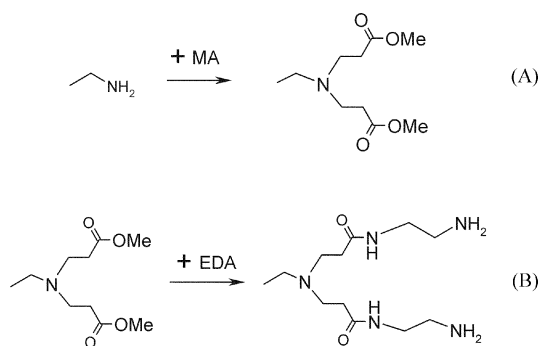
2. Propagation of Dendrimer from Silica Surface

The dendrimer building method pioneered by Tsubokawa and co-workers [Tsubokawa et al., 1998] was slightly modified to synthesize the dendrimer. PAMAM dendrimers were constructed by the repetitive addition of a branching unit to silica gel. Michael addition of MA to terminal amine generated the amino propionate ester (G0.5). Subsequent amidation of the ester moieties with EDA completed the first generation (G1). Branching occurred at the terminal amine, which is shown in Scheme 1.
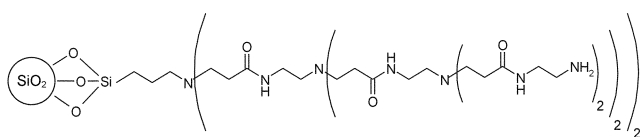
[†]To whom correspondence should be addressed.
E-mail: bu_jie@ices.a-star.edu.sg
[‡]This paper is dedicated to Professor Hyun-Ku Rhee on the occasion of his retirement from Seoul National University.

Scheme 1. Synthesis of PAMAM dendrimer: (A) Michael addition of MA to the amine termini to produce G0.5, G1.5 and G2.5; and (B) amidation of the ester moieties by EDA to generate G1 G2 and G3 dendrimers, respectively.

Scheme 2. Theoretical structure of PAMAM-SiO$_2$ dendrimer for 3rd generation (G3).

Repetition of Michael addition and Amidation reactions produced PAMAM dendrimer until third generation (G3). During the syntheses, excess reagents (MA and EDA) were fed into a batch reactor to drive reactions to completion. All reactions were carried out at 60 °C in methanol. Vacuum filtration, extraction by soxhlet apparatus, and drying in vacuo served to remove excess reagents. The theoretical structure of PAMAM-SiO$_2$ dendrimer of third generation is shown in Scheme 2.

3. Measurement of IR Spectra

During each reaction of synthesis, a series of solid samples were collected at regular intervals. In order to remove excess liquid phase, the solid sample was filtered by syringe filters and dried in vacuo at 110 °C for 2 hours. Consequently, the IR spectra of solid samples were measured on a Bruker FT-IR instrument (EQUINOX 55). In a glove box (nitrogen purging), the powder containing 2 wt% of sample in KBr was pressed to a wafer. The measurement was carried out at 100 scans and a 4 cm^{-1} resolution for background and in transmission mode. Before and during the scanning of samples, nitrogen purging to FT-IR instrument was carried out.

The amount of dendrimer grafted onto the silica surface was determined by burning the dendrimer grafted on silica from room temperature to 600 °C [Tsubokawa et al., 1998] and the weight loss was measured with a thermogravimetric analyzer (PERKIN-ELMER TGA-7).

RESULT AND DISCUSSION

1. The Extent of Reaction and IR Spectra

As described in section 2, the dendrimer synthesis process is a series of repetitive steps starting with a central initiator core. In this study, the 3-Amino-functionalized silica gel was used as starting material (G0). Consequently, Michael addition of MA to the amine
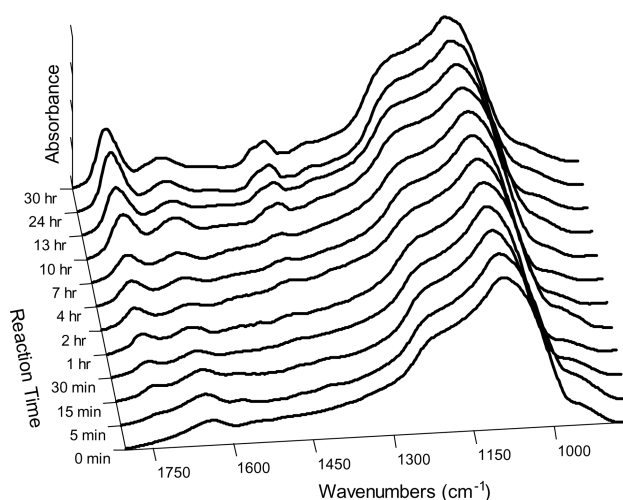

Fig. 1. FT-IR spectra of solid samples collected in synthesis step of G0 to G0.5.

group on sample G0 was carried out to produce sample G0.5. Meanwhile, a series of solid samples were collected at different interval reaction time, dried and analyzed by FT-IR. Fig. 1 presents the IR spectra of these solid samples. In order to compare the intensity of all bands observed, all IR spectra were normalized by the intensity of the strongest band at 1,080 cm^{-1}, which was assigned to Si-O-Si stretching vibration. Before reaction started (t=0), one IR band at *ca.* 1,640 cm^{-1}, which is characteristic of amine (-NH$_2$), was observed, indicating the amine on the surface of G0. When reaction was running, a new band at *ca.* 1,730 cm^{-1}, assignable to ester (-COOMe) [Wells and Crooks, 1996], appeared and increased with reaction time. Similarly, the increase in the ester band intensity can be observed in Fig. 3 and Fig. 5 which show the IR spectra of the samples, reacted with MA to form G1.5 and G2.5 dendrimers, but the increasing rate of IR intensity seems to be higher.

As shown in Fig. 2, amidation of the ester moieties on G0.5 with EDA generates G1 dendrimer, resulting in the increase in the am-
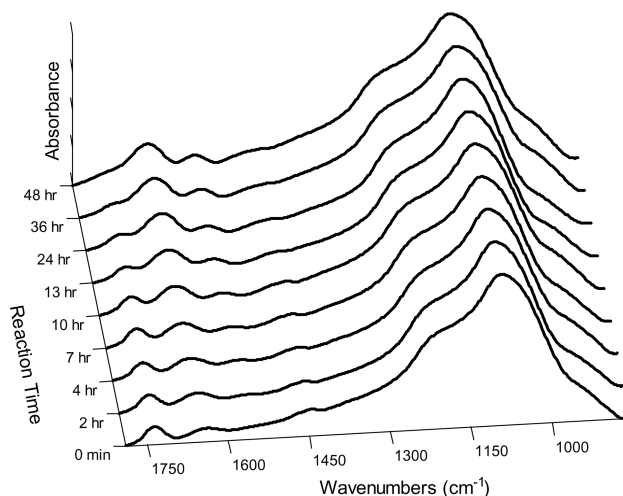

Fig. 2. FT-IR spectra of solid samples collected in synthesis step of G0.5 to G1.
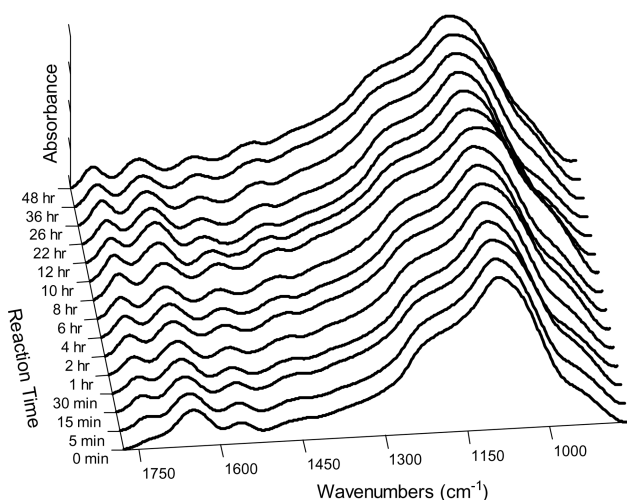
Fig. 3. FT-IR spectra of solid samples collected in synthesis step of G1 to G1.5.
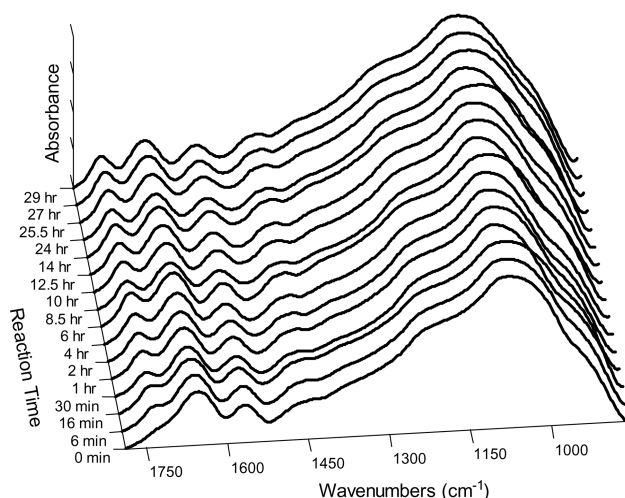

Fig. 5. FT-IR spectra of solid samples collected in synthesis step of G2 to G2.5.
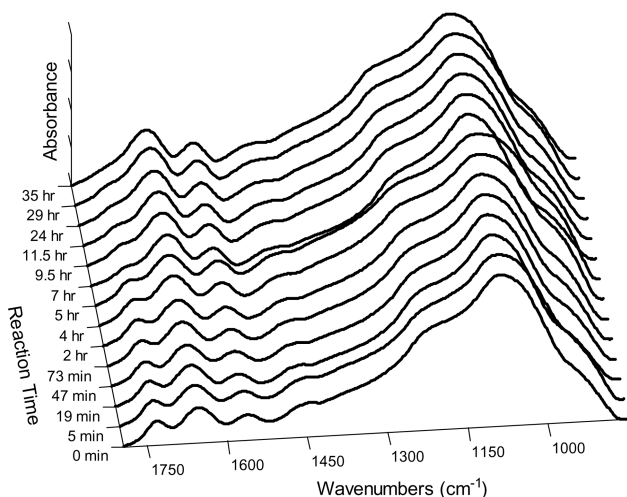

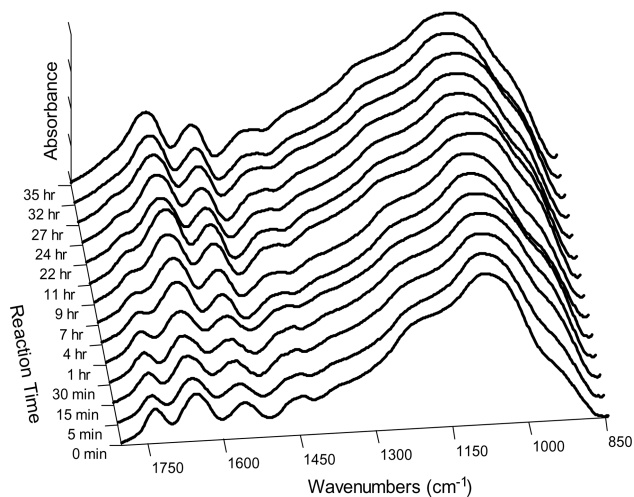Fig. 4. FT-IR spectra of solid samples collected in synthesis step of G1.5 to G2.

Fig. 6. FT-IR spectra of solid samples collected in synthesis step of G2.5 to G3.

ide band intensity and the decrease in ester band intensity. Compared to Fig. 1, two new Infrared bands at 1,655 and 1,550 cm^{-1} appeared. They were assigned to amide I and amide II groups [Wells and Crooks, 1996]. Similarly to the generation of G1, G2 and G3 dendrimers were constructed by reacting G1.5 and G2.5 samples with EDA. From Fig. 4 and Fig. 6, it was found that the ester band gradually disappeared, while the amide bands became stronger.

To ensure the completion of Michael addition and amidation carried out on the solid surface, monitoring the changes of ester band in intensity by FT-IR spectrometer is necessary. It is worth noting that at the beginning of Michael addition reaction, the intensity of the ester band increased from zero to maximum value and retained this value to the end (*cf.* Fig.1, Fig. 3 and Fig. 5). This indicates that the reaction proceeded to completion. Contrary to Michael addition, during the amidation reaction, the peak of ester decreased from the beginning and totally vanished at the end (*cf.* Fig. 2, Fig. 4 and Fig. 6), which strongly suggests that the amidation step is complete under current conditions.

2. Conversion of Reaction

The original IR spectra measured were treated and analyzed by using of OPUS software supplied by Bruker. The ester band intensity (*cf.* Fig. 1 to Fig. 6) was calculated by curve-fitting, and was plotted as a function of the reaction time in Fig. 7 and Fig. 8, which clearly demonstrate the conversion profiles of ester group in Michael addition reaction (*cf.* Fig. 7) and amidation reaction (*cf.* Fig. 8). As shown in Fig. 7, the reaction rates of Michael addition in different synthesis steps are different. The reaction rate of the Michael addition carried out on the higher generation of dendrimer is larger than that of on lower generation of dendrimer, in following order: Rate (G2-G2.5)>Rate (G1-G1.5)>Rate (G0-G0.5).

A similar tendency was observed in amidation process. As presented in Fig. 8, the disappearance rate of ester was accelerated when amidation reaction was carried on G1.5 and G2.5. These observations are in agreement with previous study [Bu et al., 2003], that the long dendritic backbone chain-arms become more flexible, thus increase the accessibility of reactant molecules resulting in the en-
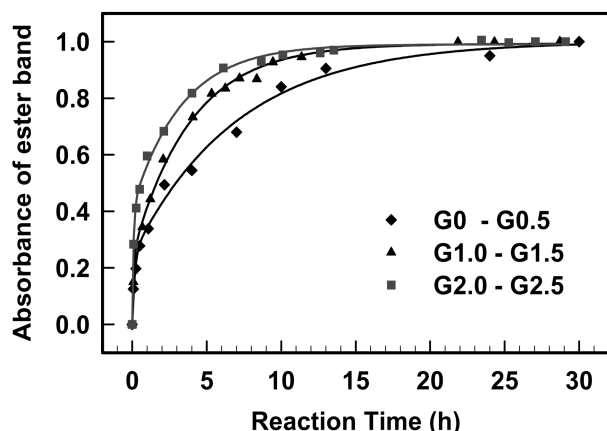
Fig. 7. The changes of ester IR band (1,730 cm^{-1}) as function of re-
action time in different synthesis steps: (◆) G0 to G0.5, (▲)
G1 to G1.5, (■) G2 to G2.5.
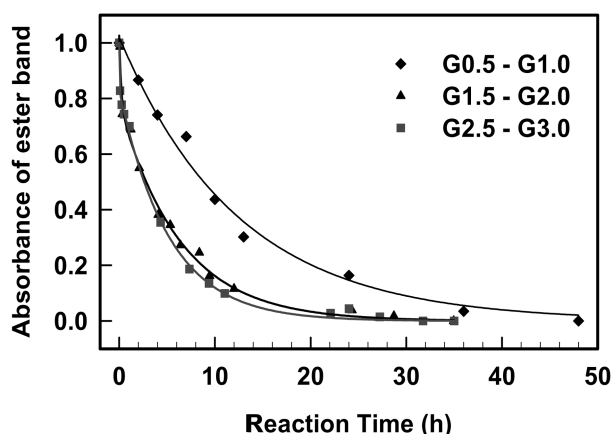

Fig. 8. The changes of ester IR band (1,730 cm^{-1}) as function of re-
action time in different synthesis steps: (◆) G0.5 to G1, (▲)
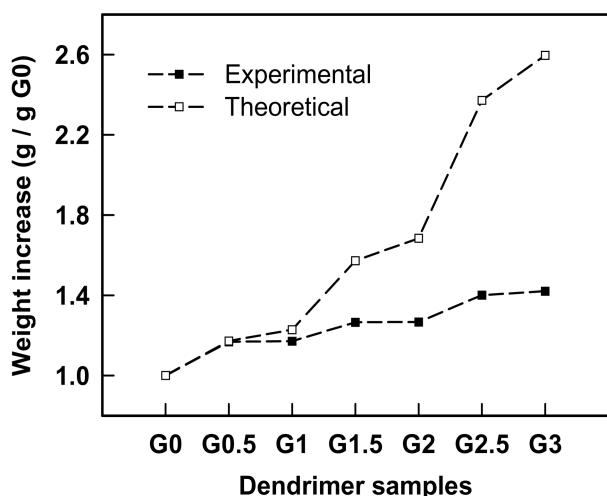G1.5 to G2, (■) G2.5 to G3.

Fig. 9. Weight increase amount of organic phase by propagation
of dendrimer on silica gel (based on one gram of G0 sam-
ple): (□) Theoretical value, (■) TGA experimental value.

hancement of reactivity.

3. Proposed Reaction Kinetics

Fig. 9 presents the grafted amount of dendrimer on silica gel, ob-
tained by TGA measurement. The weight increase of organic phase
was calculated based on one gram of G0 sample. It is found that
the grafting amount is smaller than theoretical value except G0.5
sample; implying incomplete propagation during construction. But
in this study, the FT-IR monitoring of all the synthesis process re-
veals that Michael addition and amidation reactions are complete
(*cf.* Fig. 7 and Fig. 8).

According to TGA data (*cf.* Fig. 9), the difference between the-
oretical and experimental values started from the second synthesis
step (G0.5 to G1), which is in the amidation step. Theoretically, dur-
ing amidation, one terminal amine group (-NH$_2$) in ethylene diamine
(EDA) only reacts with ester group, resulting in regeneration of am-
ine termini (*cf.* Scheme 1) and increase of the grafted amount. How-
ever, the increase of grafted amount of samples, G1, G2 and G3, is
much smaller than expected values. This implies that a side reac-
tion possibly occurs in these synthesis steps. Therefore, it is neces-
sary to investigate the reaction kinetics.

As illustrated in Scheme 3, a 'cross linking' reaction model is
proposed; two adjacent ester groups (bonding on solid phase) could
be linked by reacting with one ethylene diamine molecule, result-
ing in structural defects. Subsequently, the amidation process, con-
sisted of two series-parallel reactions, as demonstrated in Scheme 4.

According to scheme 4, the amide group on dendrimer (R) is the
desired product. If reaction (b) proceeds, two ester groups (bond-
ing on solid phase) react with one ethylene diamine molecule and
generate two methanol molecules, which are removed after drying,
causing 32 g net weight decrease. In other words, the more S gen-
erated, the smaller the actual weight increase. Therefore, this side
reaction causes structural defects and smaller grafted amount than
theoretical value, even though a complete reaction between ester
groups and amine groups was observed.

Because excessive EDA was fed in, the general representation
of these reactions is

$$E \xrightarrow[+EDA]{k_{A1}} R \qquad (R1)$$

$$R + E \xrightarrow{k_{A2}} S \qquad (R2)$$

and the rate expressions are given by

$$r_E = \frac{dC_E}{dt} = -C_E(k_{A1} + k_{A2}C_R) \qquad (1)$$

$$r_R = \frac{dC_R}{dt} = C_E(k_{A1} - k_{A2}C_R) \qquad (2)$$

Scheme 3. Structural defect caused by cross linking reaction.

Scheme 4. Amidation reaction.

Scheme 5. Michael addition of methyl acrylate to amine.

$$r_S = \frac{dC_S}{dt} = k_{A2}C_R C_E \qquad (3)$$

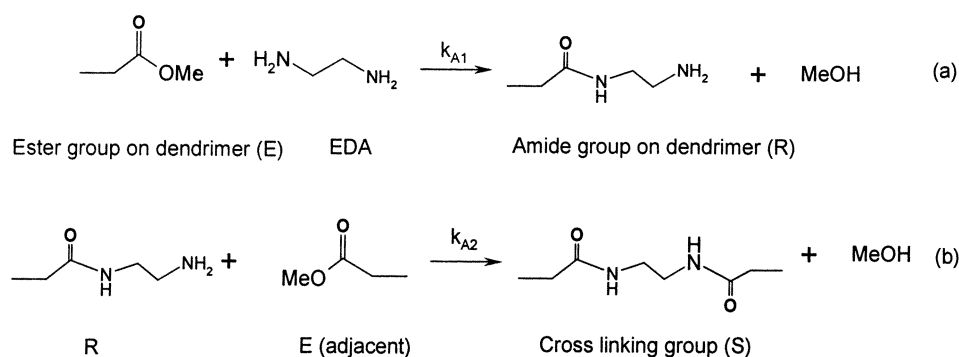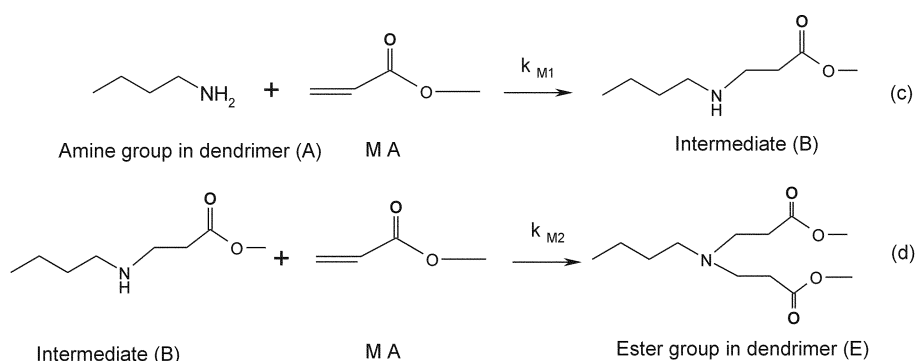In addition, Michael addition reaction steps are demonstrated in Scheme 5.

Because excessive MA was fed in, the above reactions are series pseudo-first order reactions, and the general representation of these reactions is

$$A \xrightarrow[+MA]{k_{M1}} B \xrightarrow[+MA]{k_{M2}} E \qquad (R3)$$

and the ester group on dendrimer (E) is desired product. The rate expressions are given by

$$r_A = \frac{dC_A}{dt} = -k_{M1}C_A \qquad (4)$$

$$r_B = \frac{dC_B}{dt} = k_{M1}C_A - k_{M2}C_B \qquad (5)$$

$$r_E = \frac{dC_E}{dt} = k_{M2}C_B \qquad (6)$$

Actually, the distinct band at *ca.* 1,730 cm^{-1} measured in IR spectra is assigned to the methyl ester in carbonyl (-COOMe), which exists in intermediate (B) and in the final product, the ester group in dendrimer (E) (Scheme 5). The concentration of -COOMe could be expressed by

$$C_{-COOMe} = a[1 - \exp(-k_{M1}t)] + c[1 - \exp(-k_{M2}t)] \qquad (7)$$

where a and c are constants.

Finally, all differential equations [Eq. (1) to Eq. (6)] could be solved by numerical method, followed by simulation of experimental data (*cf.* Fig. 7 and Fig. 8). Based on experimental data, all the reaction rate constants, k_1 and k_2, for each synthesis step, are calculated and listed in Table 1. The simulation curves are shown in Fig. 7 and Fig. 8 (solid lines); all simulation results match the experimental data very well.

From Table 1, the reaction rate constants, k_{M1} and k_{M2}, in Michael addition process are larger than those values in amidation process, which indicates that the amidation process is the rate-determining step for construction of PAMAM dendrimer. It is worth noting that the 'cross-linking' reaction is obvious, though the k_{A2} value of reaction (b) is smaller than the k_{A1} value of desired reaction (a) (Scheme 4). The undesired cross-linking reaction (b) reduces the amount of

Table 1. Simulation results of reaction rate constant

Synthesis procedure	Reaction step	Reaction rate constant	
		k_{M1} (h^{-1})	k_{M2} (h^{-1})
Michael addition	G0 to G0.5	1.20	0.10
	G1 to G1.5	1.50	0.21
	G2 to G2.5	7.04	0.24
		k_{A1} (h^{-1})	k_{A2}*
Amidation	G0.5 to G1	0.08	0.005
	G1.5 to G2	0.25	0.010
	G2.5 to G3	0.28	0.012

*The unit of k_{A2} is corresponding to second order reaction.

amine groups in amine termini; as a result, it has a significant cumulative effect on subsequent synthesis steps (*cf.* Fig. 9), because the subsequent Michael addition reaction (branching) occurs at the terminal amine on higher generation of dendrimers (G1 and G2).

On the other hand, we note that for the series reactions in Michael addition (*cf.* Scheme 5) the steric hindrance created by the ester group in the secondary amine moiety hinders the approach of MA molecule to the nucleophilic nitrogen center, thereby slowing down the reaction rate. Therefore, the k_{M2} value of reaction (d) is much smaller than k_{M1} (Table 1). On the other hand, the value of k_{M2} also increases at high generation due to the greater flexibility of long dendritic chain, but the increment of k_{M1} value is drastically larger than k_{M2}. These observations imply that the effect of long dendritic chain on the first step reaction is more significant than the second step reaction. However, the steric hindrance has a stronger effect on the second step reaction (d). At higher generations, the increase in the value of k_{M2} will probably become smaller, which is a possibility indicated in the observation reported by Bourque et al. [2000]. They synthesized Rh-PPh$_2$-PAMAM-SiO$_2$ catalysts and found incomplete phosphonation arising from steric crowding on third- and fourth-generation of dendrimers. In this study, the steric hindrance is not the main reason resulting in smaller grafted amount of dendrimer. As shown in Fig. 7, the two step series reactions proceed to completion if the reaction time is long enough. The study on the reaction kinetics is instrumental to the optimization of synthesis process.

CONCLUSIONS

The third generation of solid PAMAM dendrimer was synthesized by the repetitive addition of a branching unit to silica core. All synthesis steps were monitored by Infrared spectroscopy to investigate the completion of reactions.

Based on the measurements of infrared spectra, showing the changes of ester group as a function of reaction time, a reaction kinetics model was proposed and then the reaction rate constants were obtained by simulation. On the other hand, FT-IR and TGA measurements suggest that a 'cross-linking' reaction occurs in the amidation process and generates structural defects; this has a significant cumulative effect on the subsequent synthesis steps, and causes a significant reduction in the construction of dendrimer. Furthermore, the analysis of reaction rate constants indicate that due to the generation of an intermediate, Michael addition of methyl acrylate to diamine will be hindered by steric crowding.

REFERENCES

Beezer, A. E., King, A. S. H., Martin, I. K., Mitchel, J. C., Twyman, L. J. and Wain, C. F., "Dendrimers as Potential Drug Carriers; Encapsulation of Acidic Hydrophobes Within Water Soluble PAMAM Derivatives," *Tetrahedron*, **59**(22), 3873 (2003).

Bertorelle, F., Lavabre, D. and Fery-Forgues, S., "Dendrimer-tuned Formation of Luminescent Organic Microcrystals," *J. Am. Chem. Soc.*, **125**(20), 6244 (2003).

Bourque, S. C., Alper, H., Manzer, L. E. and Arya, P., "Hydroformylation Reactions Using Recyclable Rhodium-complexed Dendrimers on Silica," *J. Am. Chem. Soc.*, **122**(5), 956 (2000).

Bourque, S. C., Maltais, F., Xiao, W. J., Tardif, O., Alper, H., Arya, P.

and Manzer, L. E., "Hydroformylation Reactions with Rhodium-complexed Dendrimers on Silica," *J. Am. Chem. Soc.*, **121**(13), 3035 (1999).

Bu, J., Judeh, Z. M. A., Ching, C. B. and Kawi, S., "Epoxidation of Olefins Catalyzed by Mn(II) Salen Complex Anchored on PAMAM-SiO$_2$ Dendrimer," *Catal. Lett.*, **85**(3-4), 183 (2003).

Choi, H. C., Kim, W., Wang, D. W. and Dai, H. J., "Delivery of Catalytic Metal Species onto Surfaces with Dendrimer Carriers for the Synthesis of Carbon Nanotubes with Narrow Diameter Distribution," *J. Phys. Chem. B*, **106**(48), 12361 (2002).

Chung, Y. M. and Rhee, H. K., "Design of Silica-supported Dendritic Chiral Catalysts for the Improvement of Enantioselective Addition of Diethylzinc to Benzaldehyde," *Catal. Lett.*, **82**(3-4), 249 (2002).

Chung, Y. M. and Rhee, H. K., "Pt-Pd Bimetallic Nanoparticles Encapsulated in Dendrimer Nanoreactor," *Catal. Lett.*, **85**(3-4), 159 (2003).

Driffield, M., Goodall, D. M., Klute, A. S., Smith, D. K. and Wilson, K., "Synthesis and Characterization of Silica-supported L-Lysine-based Dendritic Branches," *Langmuir*, **18**(22), 8660 (2002).

Hecht, S. and Frechet, J. M. J., "Dendritic Encapsulation of Function: Applying Nature's Site Isolation Principle from Biomimetics to Materials Science," *Angew. Chem. Int. Edit*, **40**(1), 74 (2001).

Jang, J. G., Park, H. B. and Lee, Y. M., "Molecular Thermodynamics Approach on Phase Equilibria of Dendritic Polymer Systems," *Korean J. Chem. Eng.*, **20**, 375 (2003).

Luo, D., Haverstick, K., Belcheva, N., Han, E. and Saltzman, W. M., "Poly(ethylene glycol)-conjugated PAMAM Dendrimer for Biocompatible, High-efficiency DNA Delivery," *Macromolecules*, **35**(9), 3456 (2002).

Marsh, I. R., Smith, H. and Bradley, M., "Solid Phase Polyamine Linkers - Their Utility in Synthesis and the Preparation of Directed Libraries Against Trypanothione Reductase," *Chem. Commun.*, (8), 941 (1996).

Oosterom, G. E., Reek, J. N. H., Kamer, P. C. J. and van Leeuwen, P., "Transition Metal Catalysis Using Functionalized Dendrimers," *Angew. Chem. Int. Edit*, **40**(10), 1828 (2001).

Stiriba, S. E., Frey, H. and Haag, R., "Dendritic Polymers in Biomedical Applications: From Potential to Clinical Use in Diagnostics and Therapy," *Angew. Chem. Int. Edit*, **41**(8), 1329 (2002).

Swali, V., Wells, N. J., Langley, G. J. and Bradley, M., "Solid-phase Dendrimer Synthesis and the Generation of Super-high-loading Resin Beads for Combinatorial Chemistry," *J. Org. Chem.*, **62**(15), 4902 (1997).

Tsubokawa, N., Ichioka, H., Satoh, T., Hayashi, S. and Fujiki, K., "Grafting of 'Dendrimer-like' Highly Branched Polymer onto Ultrafine Silica Surface," *React. Funct. Polym.*, **37**(1-3), 75 (1998).

van Heerbeek, R., Kamer, P. C. J., van Leeuwen, P. and Reek, J. N. H., "Dendrimers as Support for Recoverable Catalysts and Reagents," *Chem. Rev.*, **102**(10), 3717 (2002).

Vogtle, F., Gestermann, S., Hesse, R., Schwierz, H. and Windisch, B., "Functional Dendrimers," *Prog. Polym. Sci.*, **25**(7), 987 (2000).

Wells, M. and Crooks, R. M., "Interactions Between Organized, Surface-confined Monolayers and Vapor-phase Probe Molecules. 10. Preparation and Properties of Chemically Sensitive Dendrimer Surfaces," *J. Am. Chem. Soc.*, **118**(16), 3988 (1996).

Zimmerman, S. C., Wendland, M. S., Rakow, N. A., Zharov, I. and Suslick, K. S., "Synthetic Hosts by Monomolecular Imprinting Inside Dendrimers," *Nature*, **418**(6896), 399 (2002).